Chem Soc Rev

REVIEW ARTICLE

Recent advancements in membrane-free redox flow batteries

Xiao Wang, Rajeev K. Gautam and Jianbing "Jimmy" Jiang [iD] *

Membrane-free redox flow batteries (RFBs) are promising energy-storage technologies that present an innovative solution to address the critical need for sustainable and efficient energy systems. This review provides a detailed examination of membrane-free RFBs, focusing on recent technological advances and design optimization. Moreover, it highlights the growing importance of membrane-free designs for achieving higher efficiency and scalability in energy-storage systems. These designs offer significant improvements in terms of electrolyte concentration, Coulombic efficiency, and flow management, underscoring the potential of these systems for advanced energy-storage solutions. We explore the utilization of immiscible electrolyte solvents and the engineering of laminar flow dynamics to achieve efficient electrolyte separation without traditional ion-exchange membranes. The article discusses metal-free and metal-phase aqueous/nonaqueous and nonaqueous/nonaqueous immiscible solvent-based RFBs; laminar flow-based RFBs; single-phase co-laminar flow batteries; liquid/solid membrane-free RFBs; and triphasic membrane-free RFBs, highlighting their unique design features and operational benefits, as well as their potential and challenges in energy-storage applications. Key parameters such as the coulombic efficiency, self-discharge, flow dynamics, and impedance are analyzed to provide a comprehensive understanding of the performance metrics critical for the development of next-generation membrane-free RFBs. We provide valuable references for developing membrane-free RFBs and highlight their significance, technological advancements, and implications for future energy-storage applications. In the context of global energy transitions, the research and development of membrane-free batteries will provide crucial technical support for achieving sustainable energy development.

Department of Chemistry, University of Cincinnati, P.O. Box 210172, Cincinnati, Ohio 45221-0172, USA. E-mail: jianbing.jiang@uc.edu

Xiao Wang received his Master's degree at Qingdao University of Science and Technology. He is now a PhD candidacy under the supervision of Professor Jianbing "Jimmy" Jiang at the University of Cincinnati. His research mainly focuses on redox flow batteries and Li metal batteries.

Xiao Wang

Dr Rajeev Gautam obtained his PhD in Materials Science from the Indian Institute of Technology Kanpur, focusing on the development of nanostructured materials for PEM fuel cells. Dr Gautam, recipient of the SERB-DST Young Scientist Fellowship, to conduct independent research on vanadium redox flow batteries. Later he joined Dr Jiang's group as a postdoctoral fellow at the Department of Chemistry, University of Cincinnati. His research interests include aqueous and non-aqueous redox flow batteries, slurry batteries, membrane-free biphasic batteries, and Li metal batteries.

Rajeev K. Gautam

This journal is © The Royal Society of Chemistry 2025

Chem. Soc. Rev., 2025, **54**, 5895–5911 | **5895**

1. Introduction

The growing energy crisis has resulted in the development and utilization of new energy sources.[1,2] Owing to their clean and renewable nature, wind and solar energies have attracted significant attention.[3–5] However, wind and solar power generation depends on natural conditions, characterized by unpredictability and intermittency, thereby limiting their large-scale application.[6] Fluctuations in the energy supply to the grid hinder the stability and reliability of these power systems. To achieve a balanced energy supply, reliable large-scale energy-storage systems are required to store energy during periods of low demand and release it during peak demand.[7]
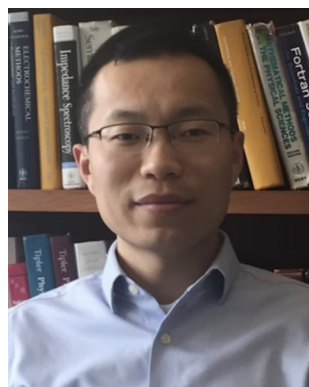
Among various energy-storage solutions, redox flow batteries (RFBs) have emerged as a promising option owing to their unique advantages. RFBs, particularly vanadium RFBs, have a large capacity and long cycle life.[8] In addition, RFBs have a simple structure and are easily maintained, rendering them attractive for practical applications.[9–11] The operating principle of RFBs is based on the redox reactions of active species dissolved in electrolytes stored in external tanks. The system capacity can be flexibly adjusted by changing the tank size. This design provides high storage flexibility and offers significant advantages in managing large-scale energy-storage demands. However, the commercialization of RFBs faces several challenges. First, the cost of vanadium RFBs is high. Vanadium is a rare metal, and its extraction and refining processes are complex and costly, which significantly increases the overall cost of RFBs. Second, the corrosiveness of the vanadium electrolyte accelerates the aging and failure of internal components, contributing to maintenance costs and shortening the lifespan of the battery.[12] Third, current RFB designs rely on expensive ion-exchange membranes (approximately 40% of the total system cost) to prevent cross-contamination between electrolytes. These ion-exchange membranes also have a limited lifespan, limiting the large-scale employment of RFBs.[13,14]

To address these issues, researchers have proposed membrane-free batteries. Marcilla and coworkers provided a comprehensive review on the evolution of membrane-free RFBs, highlighting key advancements and the economic and technical drivers behind their development, particularly cost reduction through membrane elimination and immiscible electrolyte use.[15] By eliminating ion-exchange membranes through innovative designs, membrane-free batteries can significantly reduce costs[16,17] while mitigating the negative impact of electrolyte corrosiveness. To prevent cross-contamination, the physical and chemical differences between phases are exploited to achieve the spontaneous separation of electrolytes. This innovative concept also enhances the overall battery performance and stability.[18,19] Membrane-free RFBs offer several significant benefits that make them particularly appealing for large-scale energy storage applications. One of the primary advantages is the reduction in cost, as these systems eliminate the need for expensive ion-exchange membranes, which are a major cost component in traditional RFBs. This also simplifies the design and reduces maintenance requirements, since the absence of membranes removes a common point of failure due to fouling or degradation over time. In addition, membrane-free RFBs minimize issues related to reactant crossover, which can degrade performance in conventional systems; by using fluid dynamics to separate the reactants, these batteries maintain higher efficiency and stability over long periods. Furthermore, without the resistance associated with ion transport across a membrane, membrane-free systems can achieve higher energy efficiencies, making them particularly suitable for applications that require frequent charge and discharge cycles, such as grid stabilization and renewable energy integration. When compared to other energy storage technologies such as lithium-ion or solid-state batteries, membrane-free RFBs stand out for their scalability and flexibility, especially in large-scale applications where cost, durability, and environmental impact are critical considerations.

However, a series of technical challenges require in-depth research for the development of membrane-free batteries. First, appropriate electrode materials and electrolyte systems must be selected to achieve efficient energy conversion and storage, which is a critical issue in membrane-free battery research. Second, the structural design of batteries must be optimized to enhance their energy density and cycle life.[20]

This review aims to comprehensively discuss membrane-free batteries by considering the historical background, scientific basis, working principles, and key technologies of membrane-free batteries. Subsequently, we examine the recent advances in their design and utilization and analyze the challenges and solutions for their practical applications. Finally, future development directions for membrane-free batteries are discussed, highlighting their potential and prospects for large-scale energy-storage systems. This review provides valuable references for

Dr Jimmy Jiang is currently an Associate Professor in the Department of Chemistry at the University of Cincinnati. He earned his BS from Jiangnan University in 2007 and MS from East China University of Science and Technology (advisor: He Tian) in 2010. He obtained his PhD from North Carolina State University (advisor: Jonathan Lindsey) working on tetrapyrrole compounds for energy applications. In 2015, he joined Yale University as a Postdoctoral Associate and then an Associate Research Scientist in the Department of Chemistry and Yale Energy Sciences Institute, working with Professors Gary Brudvig and Robert Crabtree on organometallic materials for small molecule activation and energy storage. Jimmy started his independent career as an Assistant Professor in the Department of Chemistry at the University of Cincinnati in 2018 and was tenured in 2022. He received the NSF CAREER award in 2021, and was named an Alfred P. Sloan Fellow in 2022.

Jianbing "Jimmy" Jiang

5896 | *Chem. Soc. Rev.*, 2025, **54**, 5895–5911

This journal is © The Royal Society of Chemistry 2025

research on membrane-free batteries, which have great potential as emerging energy-storage technologies, and offers guidance for future practical applications. In the context of global energy transitions, the research and development of membrane-free batteries will provide crucial technical support for achieving sustainable energy development.

2. Principles of membrane-free RFBs

Conventional membrane-based RFBs use a membrane, often an ion-exchange membrane, to separate the anolyte and catholyte compartments. This membrane enables selective ionic conduction while preventing mixing of the two redox species. During operation, oxidation reactions occur at the anode while reduction reactions occur at the cathode. The membrane facilitates the movement of ions (e.g., H^+ or OH^-) to balance the charge without mixing the anolytes and catholytes.[21] Despite their effectiveness, these membranes can add significant cost and complexity to the system. Over time, membrane fouling and degradation can result in reduced efficiency and increased maintenance requirements.[22,23]

Membrane-free RFBs eliminate the membrane by employing two distinct methodologies: (1) precise engineering of laminar flow dynamics within the battery, and (2) exploiting the immiscibility of the electrolyte solvents (Fig. 1A and B, respectively). These systems establish a stable interface between the anolyte and catholyte by optimizing parameters, such as the flow rate and channel geometry, effectively preventing the mixing of two phases. Similar to in conventional RFBs, oxidation and reduction reactions occur at the respective electrodes. However, in membrane-free systems, the separation of reactants is accomplished through controlled laminar flow or by exploiting the inherent immiscibility of fluids, which effectively resist mixing.
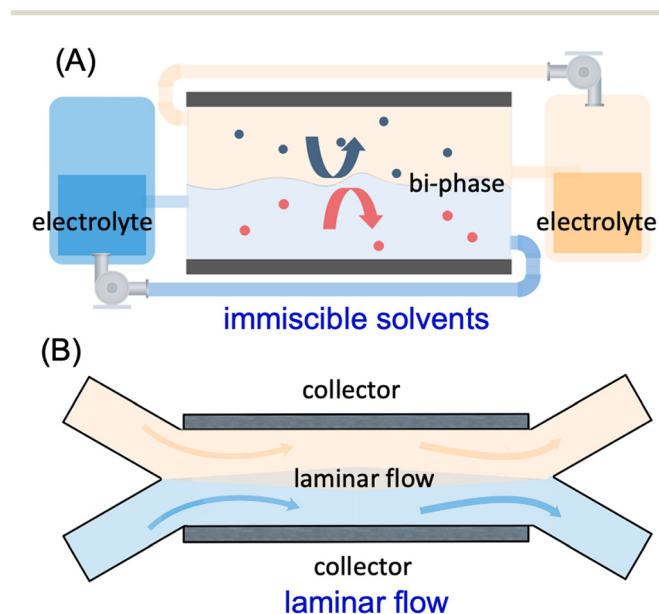

Fig. 1 (A) Immiscible solvent-based and (B) laminar flow-based membrane-free flow batteries.

In addition to operational considerations, the materials chemistry of membrane-free RFBs plays a critical role in their performance and stability. The selection of redox-active materials (redoxmers) requires careful consideration of their chemical properties, such as redox potential stability, solubility, and reactivity. For instance, molecules with reversible redox behavior and high solubility in the chosen electrolyte are preferred to maximize energy density and Coulombic efficiency. Electrolyte composition is equally important, as solvent polarity, dielectric constant, and viscosity influence ion transport and phase separation. The significant differences in the properties of the solvents used – including density, mutual solubility (miscibility), and substantial variations in solubility for the same solute – ensure the formation of a stable biphasic system, effectively preventing reactant crossover. Furthermore, molecular design strategies can be employed to optimize redox-active species. Modifications, such as introducing electron-donating or withdrawing groups, can adjust redox potentials and enhance solubility, conductivity, and electrochemical stability. For example, redox-active organic molecules, such as TEMPO and methyl viologen, can be functionalized to improve their performance in nonaqueous or biphasic systems. In the context of ion transport, the role of electrolyte additives, such as ion-pairing agents or stabilizers, is critical in mitigating self-discharge and maintaining long-term stability.

Eliminating the membrane simplifies the overall design and construction of the battery, potentially reducing the complexity of its assembly and operation. It can also significantly reduce material costs because of the expense of high-performance ion-exchange membranes. Additionally, the reduced need for maintenance and replacement of membranes lowers the long-term operational costs. Membrane-free RFBs may offer enhanced durability and longevity because they are not susceptible to issues such as membrane fouling or chemical degradation. By avoiding membrane resistance, these systems can achieve higher energy efficiencies, particularly at high current densities, where the membrane resistance is more pronounced.

3. Types of membrane-free RFBs

3.1. Liquid/liquid membrane-free RFBs

Membrane-free RFBs can employ a phase-separated liquid/liquid interface, thus eliminating the need for solid membranes. Similar to traditional RFBs, these systems use liquid electrolytes as energy carriers. However, phase separation is achieved through differences in solvent properties. Liquid/liquid membrane-free RFBs represent the initial and most fundamental form of phase-separated biphasic flow batteries.[17]

3.1.1. Aqueous phase-containing membrane-free flow batteries. Aqueous phase-containing membrane-free batteries are currently mainstream in biphasic systems. In these systems, water, which is inexpensive and has a high ionic conductivity, is typically used as the solvent for one phase of the biphasic system. The other phase employs an immiscible organic solvent, ionic liquid, or liquid oligomer (polymer) to achieve spontaneous phase separation. Alternatively, phase separation

This journal is © The Royal Society of Chemistry 2025

Chem. Soc. Rev., 2025, 54, 5895–5911 | 5897

Table 1 Key parameters in aqueous phase-containing membrane-free flow batteries

Solvents	Redoxmer	Salt	SOC^i	Energy density (W h L^{-1})	Flow	No. of cycles	Current density (mA cm^{-2})	Battery voltage (V)	Conc. (mM)	Year	Ref.
H$_2$O/PYR$_{14}$TFSI	H$_2$Q^a/pBQ^b	HCl	20%	2.4	No	75	0.2	1.4	20	2017	17
H$_2$O/[P$_{44\,414}$]Cl	TEMPO^c/MV^d	Na$_2$SO$_4$	20%	15.3	No	20	0.16	1.35	20	2018	24
H$_2$O/PEG^e	TEMPO/MV	Na$_2$SO$_4$	20%	1.6	No	550	0.5C	1.23	100	2020	25
H$_2$O/PEG	FcNCl/MV	(NH$_4$)$_2$SO$_4$	20%	∼0.9	Yes	100	2.8	1.1	100	2023	26
H$_2$O/butyl acetate	Zn/Fc	Aliquat 336	NA^j	0.17	No	20	0.1	1.35	0.05	2017	27
H$_2$O/(60/40:EA/IL)	Fe(acac)$_3$/FeCl$_2$	NaCl	NA	NA	Yes	25	0.08	1.2	0.05	2018	28
H$_2$O/TEGDME^f	Zn/TEMPO	LiTFSI, ZnSO$_4$, MgSO$_4$	∼100%	20	Stir	150	NA	1.1	1500	2020	29
H$_2$O/CH$_2$Cl$_2$	Zn/PTZ^g	KPF$_6$, TBAPF$_6$	NA	19	No	202	∼12	1.53	100	2021	30
H$_2$O/acetonitrile	Zn/TEMPO	ZnSO$_4$, MgSO$_4$, NH$_4$PF$_6$	NA	18	Yes	190	8.5	1.52	500	2021	31
H$_2$O/CH$_2$Cl$_2$	Zn/Br$_3^-$	ZnBr$_2$, TBABr$_3$^{h}	NA	NA	No	260	2	1.7	1500	2024	32
H$_2$O/Water	Zn/FcNCl	ZnCl$_2$, LiTFSI	31.1%	∼2.6	Yes	30	15	1.12	100	2024	33

^{a} Note: H$_2$Q, hydroquinone. ^{b} pBQ, parabenzoquinone. ^{c} TEMPO, 2,2,6,6-tetramethyl-1-piperidinyloxy. ^{d} MV, methyl viologen. ^{e} PEG, polyethylene glycol. ^{f} TEGDME, tetraethylene glycol dimethyl ether. ^{g} PTZ, phenothiazine. ^{h} TBABr$_3$, tetrabutylammonium bromide. ^{i} SOC: state of charge. ^{j} NA: data not published in the original study.

is induced in otherwise miscible solvents such as acetonitrile and water by methods such as salting-out. Table 1 lists the solvent details, supporting salt, energy density attained, and other parameters of key aqueous phase-containing membrane-free flow batteries.

The concept of phase-separated membrane-free batteries was introduced by Marcilla and colleagues in 2017.[17] The paper proposed the use of two immiscible electrolytes to form a biphasic system, in which the interphase functioned as a natural barrier, thus eliminating the need for a physical membrane. The authors demonstrated this concept using an HCl solution of hydroquinone and a hydrophobic ionic liquid (PYR$_{14}$TFSI) containing dissolved parabenzoquinone. A stable interface was maintained between the two immiscible phases, preventing crossover and enabling the battery to effectively function without a membrane. This system exhibited a limited capacity retention of 50% after 30 cycles and a power density of only 0.6 mW cm^{-2}, which are significantly lower than those of membrane-based RFBs. However, this innovation was significant because it showcased a viable method for reducing costs and improving the practicality of RFBs by removing the dependence on expensive ion-exchange membranes (Fig. 2A and B).

Following this work, Marcilla and colleagues[24] optimized the biphasic membrane-free system by selecting Na$_2$SO$_4$ as the supporting salt due to its moderate salting-out effect and neutral pH, which helped to stabilize the phases and maintain the chemical integrity of the electrolytes. They also carefully screened and selected low-toxicity ionic liquids to ensure environmental safety and reduce the potential hazards associated with battery operation. Additionally, they adopted more established redox-active materials, such as methyl viologen and 2,2,6,6-tetramethyl-1-piperidinyloxy (TEMPO), which demonstrated better performance and stability in the biphasic system. Despite these optimizations, the battery only achieved 20 cycles without degradation, which is insufficient in terms of long-term stability. However, the area-specific resistance of the battery, at just 7%, was far superior to the 70% typically observed in conventional membrane batteries, highlighting the design advantages of membrane-free biphasic batteries.

Marcilla's group[25] further developed this concept by replacing the ionic liquid with a water/oligomer (polyethylene glycol) system, which significantly improved the battery performance without altering the overall structure. This new system demonstrated excellent long-term cycling stability, with a capacity retention of 99.9% over 550 cycles and an exceptional round-trip efficiency of 70% (Fig. 2C and D). In another study,[26] a more environmentally friendly and neutral electrolyte condition was achieved by replacing Na$_2$SO$_4$ with (NH$_4$)$_2$SO$_4$, and the battery performance was further optimized by adjusting the salt concentration and flow rates.

The series of works by Marcilla's group pioneered the concept of biphasic membrane-free batteries and progressively optimized the systems to enhance battery performance. However, the entire membrane-free biphasic battery system requires improvement. The first objective for the development of biphasic membrane-free system is to broaden the electrochemical window of the battery. This can be achieved by exploiting the ability of the nonaqueous solvent to withstand extreme voltages to increase the working voltage. The working voltages of the batteries in the aforementioned studies were all less than 1.4 V. This value is consistent with that of aqueous batteries and does not leverage the advantages of nonaqueous solvents. Second, most of the electrolyte concentrations were 0.1 M. Compared with vanadium RFBs, which often use concentrations in excess of 1 M, these low concentrations greatly reduce competitiveness. Thus, the concentration must be improved. Third, the complexity of the system must be reduced. There are two distinct types of liquids in biphasic membrane-free systems. The active materials in the positive and negative electrodes must be completely soluble in one phase and completely insoluble in the other, which significantly increases the difficulty of screening the active materials. Fourth, the utilization rate of active materials must be improved. The ultralow utilization rate of the active materials (<50% state of charge (SOC)) may have masked significant decay in the batteries.

3.1.2. Metal-containing aqueous membrane-free flow batteries. Zn is one of the most widely studied battery anode materials. It exhibits excellent stability, and its compatibility with common cathode compounds enables battery voltages to easily exceed 1.5 V.[32,34] Scientists have simplified biphasic membrane-free batteries by replacing the active materials in

5898 | Chem. Soc. Rev., 2025, **54**, 5895–5911

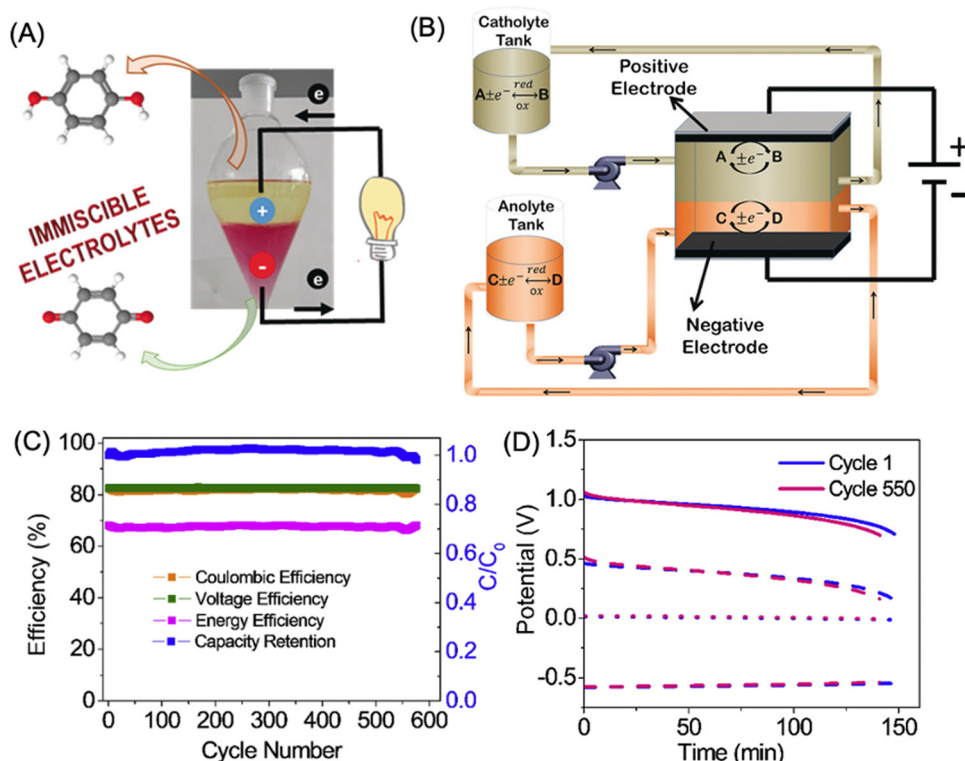This journal is © The Royal Society of Chemistry 2025

Fig. 2 (A) Schematic of a membrane-free battery with immiscible redox electrolytes. (B) Horizontally designed membrane-free biphasic flow battery and redox cyclability. (C) Efficiency and capacity retention (C/C_0) vs. cycle number of a water/oligomer (PEG1000) biphasic battery. (D) Individual potential profiles during cycling when the water/PEG1000 biphasic battery was fully charged at a specific C-rate. Reproduced with permission from ref. 17. Copyright 2017, John Wiley & Sons.

either the aqueous or nonaqueous phase with a metallic Zn electrode. This approach simplifies the system and reduces the construction complexity, because the metal avoids the risk of negative electrode crossover, thus requiring only the screening of cathode materials.

A significant advancement in this field was the work of Meng *et al.*,[29] who introduced a stirred, self-stratified battery designed for large-scale energy storage. This battery employed a gravity-driven, self-stratified architecture comprising a solid Zn anode, an aqueous electrolyte, and an organic catholyte (Fig. 3A). They innovatively used the salting-out effect to achieve phase separation between the aqueous and organic phases, which was crucial for maintaining the integrity and functionality of the battery. The salting-out effect was used to pull the polar organic solvent (tetraethylene glycol dimethyl ether (TEGDME)) out of the aqueous phase. Specifically, by adding $MgSO_4$ to a water–TEGDME mixture, TEGDME is salted-out to form a separated organic phase. This approach ensured that the organic catholyte remained separated from the aqueous electrolyte, preventing self-discharge and maintaining high ionic conductivity in both phases. The active material in the catholyte was 1.5 M TEMPO. Notably, the performance of this self-stratified battery was significantly improved by agitation (stirring). The battery achieved a TEMPO utilization of 94%, volume energy density of 20 W h L^{-1}, and a stable capacity for over 150 cycles at a 100% depth of discharge during a two-

month cycling test (Fig. 3B). However, the stirred mode could not overcome the limitations of static batteries, because the reaction and energy storage chambers remained together.
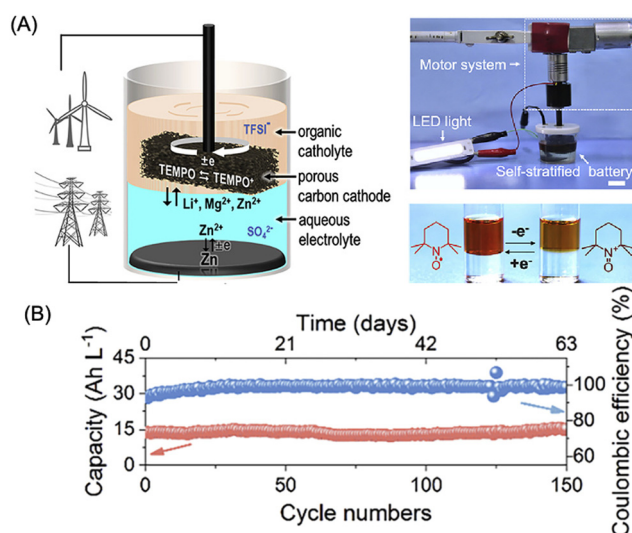

Fig. 3 (A) Schematic illustration and digital photographs of stirred self-stratified battery. (B) Cycling performance of a 20 W h L^{-1} stirred self-stratified battery. Reproduced with permission from ref. 29. Copyright 2020, Elsevier.
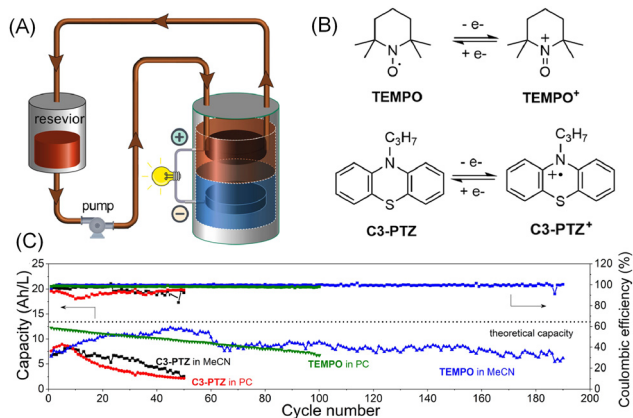
Fig. 4 (A) Schematic illustration (B) battery reaction and (C) cycling performance of a membrane-free aqueous/nonaqueous hybrid RFB. Reproduced with permission from ref. 31. Copyright 2022, Elsevier.

and the catholyte was a solution of TEMPO (0.1 M) or C3-PTZ with 0.5 M tetrabutylammonium hexafluorophosphate (TBAPF$_6$) in propylene carbonate or acetonitrile. Under ambient-flow conditions, the battery attained a capacity retention of 94.5% over 190 charge–discharge cycles, with a Coulombic efficiency (CE) of >99% at a current density of 8.54 mA cm^{-2} (Fig. 4C). Self-discharge at the full SOC of the membrane-free RFB was negligible (potential drop = 0.78 mV h^{-1}). The success of this membrane-free flow battery under dynamic conditions provided a new avenue for detailed mechanistic studies and practical applications of RFBs in cost-effective energy-storage systems.

Another study explored the stability of the cathode compounds that inevitably dissolved in the anolyte, with the aim of ensuring the robustness and longevity of the system.[31] *In situ* infrared spectroscopy was used to investigate the impact of trace amounts of miscible solvents on the stability of battery materials (Fig. 5A and B). The results showed that the different active materials responded differently to the presence of trace water; C3-PTZ was significantly affected, whereas TEMPO remained more stable (Fig. 5C). The results of the study provided new insights into the selection of active materials.

Yang *et al.*[32] further advanced this field by developing an ultralow self-discharge aqueous/organic membrane-free battery using CH$_2$Cl$_2$ and tetrabutylammonium bromide added to a ZnBr$_2$ electrolyte solution (Fig. 5D). The biphasic membrane-free battery minimized Br$_2$ crossover-induced self-discharge by confining polybromide in the organic phase. At 90% SOC, the
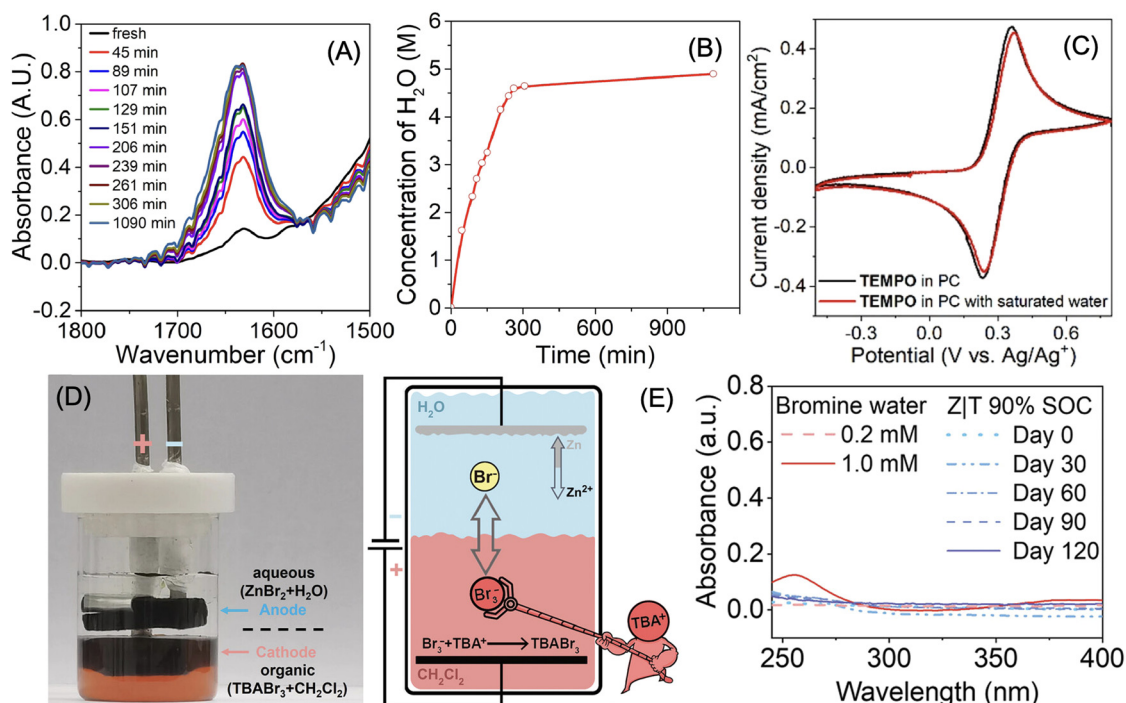
Thus, this design failed to exploit the advantages of decoupling energy and power of the flow battery.

Jiang and coworkers demonstrated the first successful operation of a membrane-free RFB under authentic flow conditions.[31] Their study presented a biphasic flow battery with a high capacity that employed the organic compounds TEMPO and phenothiazine (C3-PTZ) in the organic phase and Zn in the aqueous phase (Fig. 4A and B). The anolyte was a ternary aqueous electrolyte comprising ZnSO$_4$ (0.5 M), MgSO$_4$ (1.8 M), and NH$_4$PF$_6$ (0.3 M),

Fig. 5 (A) Evolutive Fourier-transform infrared spectra of 50 mM TEMPO in 0.5 M TBAPF$_6$/acetonitrile and (B) concentration of H$_2$O in the nonaqueous electrolyte over time. (C) The CV curves of TEMPO before and after long-term storage under the influence of saturated water. (D) Photograph and schematic illustration of a membrane-free aqueous/nonaqueous hybrid RFB. (E) UV–visible spectra of Br$_2$/water (1 and 0.2 mm) and aqueous phase of 0.5 m ZnBr$_2$|tetrabutylammonium bromide (*Z*|*T*) (Days 0, 30, 60, 90, and 120) at 90% SOC. Reproduced with permission from ref. 32. Copyright 2024, John Wiley and Sons.

battery demonstrated an open-circuit voltage drop of only 42 mV after 120 days and a capacity retention of 95.5% (Fig. 5E), outperforming previously reported liquid active-material batteries. The battery achieved over 500 cycles with nearly 100% CE and significant capacity retention, demonstrating a cost-effective and scalable design for long-term energy storage. This innovative approach highlights the potential of regulating material crossover in liquid-based batteries to realize extended operation and stable performance.

Compared to metal-free membrane-free biphasic systems, systems using Zn anodes exhibit a higher voltage, deeper charge–discharge (higher SOC), and increased concentration. These improved parameters contribute to the overall energy density of the battery. Consequently, the energy density of most Zn anode batteries can attain 15 W h L^{-1} (with reported values of 15.6, 18.7, and 20.0 W h L^{-1}[29–31]), which is nearly 25% higher than the maximum reported value of approximately 12 W h L^{-1} for systems without Zn.[26]

Recent studies have further expanded the development of aqueous biphasic membrane-free RFBs. Senthilkumar et al. introduced a membrane-free Zn hybrid RFB employing a "water-in-salt" aqueous biphasic system (WIS-ABS), composed of ZnCl$_2$ and LiTFSI phases as a unique approach to overcome the self-discharge issue inherent in membrane-free designs. The system demonstrated excellent phase separation, achieving a capacity retention of 96.4% after 30 cycles.[33] The system demonstrated excellent phase separation, achieving a capacity retention of 96.4% after 30 cycles. By employing immiscible electrolytes with Zn salts and a ferrocene derivative, this battery effectively mitigates self-discharge and consistently achieves nearly 100% Coulombic efficiency over 2000 cycles under static conditions. Furthermore, by shifting to a flowing system, they achieve significant improvement in catholyte utilization, reaching up to 95%, and maintain a Coulombic efficiency above 95% during cycling. The innovative use of WIS-ABS allows for stable cycling with high capacity retention, making it a notable advancement in all-aqueous, membrane-free systems that balances electrochemical performance with practical operational stability. Similarly, Ejigu et al. developed an all-aqueous biphasic interface (ABI) system using LiCl and LiTFSI, demonstrating effective phase separation and reduced crossover, achieving a Coulombic efficiency exceeding 99% in Zn-halide RFBs.[35] The emergence of water/water membrane-free biphasic systems has reduced reliance on organic solvents to some extent, presenting a promising new direction with significant potential for further exploration and development.

However, there are significant concerns associated with Zn-based systems owing to inherent issues with Zn. For example, large currents and a lack of necessary control measures result in substantial dendrite formation. In experimental batteries, the height of the solution far exceeds the height of the dendrites, preventing immediate performance issues, which is primarily due to the excess amount of Zn used in the anode. However, as the system scales up to the industrial level, the proliferation of dendrites will inevitably affect the capacity and CE. Additionally, using soluble Zn salts as essential participants in the redox

process increases the acidity of the electrolyte. This results in hydrogen evolution, which contributes to a lower CE in certain battery systems; an issue that urgently needs to be addressed.[36] To circumvent the limitations of Zn anodes, some studies have explored alternative electrode materials. The study by Hou et al. presents a membrane-free chlorine RFB that uses Cl$_2$/Cl$^-$ as positive redox couple and Na$_3$Ti$_2$(PO$_4$)$_3$/NaTi$_2$(PO$_4$)$_3$ as negative redox couple.[37] This system achieves an impressive energy density of 125.7 W h L^{-1} and maintains high energy efficiency ($>$91%) at 10 mA cm^{-2}, owing to the high solubility of Cl$_2$ in carbon tetrachloride (CCl$_4$). The immiscibility of CCl$_4$ and NaCl solutions enables a membrane-free design by preventing cross-contamination. This unique approach avoids the high costs associated with ion-exchange membranes while utilizing low-cost, abundant raw materials. The design demonstrates scalability and cost-effectiveness, making it suitable for grid-scale applications where economic and operational efficiency are paramount. Hou et al.'s work represents an important advancement in cost-effective, membrane-free systems that leverage naturally abundant chemistries to meet large-scale storage requirements. Jiang and coworkers developed an air-stable membrane-free Mg RFB based on an aqueous/nonaqueous biphasic system.[38] The design featured a Mg metal anode with a protective Mg^{2+}-conductive polymer interface and two organic catholytes, TEMPO and C3-PTZ, achieving a high cell voltages of 2.07–2.12 V, stable capacity retention ($>$93% over 500 cycles under flow conditions), and power densities exceeding 190 mW cm^{-2}. This study further demonstrates the feasibility of aqueous/nonaqueous biphasic systems for high-energy, membrane-free RFB applications. In addition, some researchers have successfully integrated the membrane-free battery concept with other energy technologies, achieving promising results. Zhang et al. developed a membrane-free RFB based on a thermally regenerative electrochemical cycle (TREC), which stores electricity while simultaneously managing the waste heat produced by perovskite solar cells.[39] This system employs Zn/Mn-based redox couples and is uniquely designed to address multiple functions within a single system: it stores electrical energy, cools the solar cell to prevent efficiency losses, and converts waste heat into electricity. The choice of redox couples with a negative temperature coefficient allows for efficient heat management and thermoelectric power generation, enhancing the overall energy output. The TREC-based RFB also minimizes costs by eliminating the need for an ion-selective membrane, which not only reduces material costs but also simplifies the design and improves thermal resilience.

3.1.3. Nonaqueous/nonaqueous membrane-free flow batteries. Nonaqueous/nonaqueous membrane-free flow batteries are constructed using two nonaqueous solvents. Compared with systems involving water, the wider electrochemical window of nonaqueous solvents enables greater flexibility in the selection of active materials. Solvents with high electrochemical stability, such as ionic liquids and carbonate esters, are often paired with alkali metals such as Na, Li, and Mg. This combination significantly enhances the battery voltage.

Most research on nonaqueous membrane-free batteries has focused on static cells. For example, researchers have used

This journal is © The Royal Society of Chemistry 2025

Chem. Soc. Rev., 2025, **54**, 5895–5911 | **5901**

differences in solvent polarity and density to select biphasic systems in Li–S batteries. Low-polarity solvents, typically ethers such as dibutyl ether or diethyl ether, are used as electrolytes with Li anodes. Because these solvents do not dissolve lithium polysulfides, they effectively function as a "membrane" to suppress crossover, thereby outperforming several membrane-based batteries in terms of performance.[20,40] Zhao and colleagues[41] successfully constructed a dual-nonaqueous system using TEGDME and nonafluoro-1,1,2,2-tetrahydrohexyl-trimethoxysilane (NFTOS) with Li salt. Owing to the excellent compatibility of NFTOS with Li metal, Li was used as the anode, and a mature anthraquinone material, 2-ethylanthraquinone, was used as the cathode. The biphasic system was stable under different charge–discharge states, with no significant crossover, as evidenced by UV-visible spectroscopy (Fig. 6A–C). This setup achieved a voltage of 2.37 V at a redoxmer concentration of 0.2 M, elevating the energy density to 21.4 W h L^{-1}.

Although researchers have attempted to construct static membrane-free battery systems, the combination of nonaqueous solvents with Li–metal anodes and organic compounds is highly suitable for RFBs. Jiang and coworkers[42] developed a high-voltage and high-energy membrane-free nonaqueous Li-based organic RFB. This battery employed an all-organic biphasic system with a Li–metal anode and utilized LiClO$_4$ (1.5 M) for the salting-out effect to achieve phase separation. The anode solvent was an ionic liquid, 1-butyl-1-methylpyrrolidinium bis-(trifluoromethylsulfonyl)imide (BMP-TFSI), while the cathode solvent was fluoroethylene carbonate (FEC) (Fig. 6D). They reported the excellent electrochemical performance of the Li‖Tri-TEMPO flow battery, achieving a discharge voltage and energy density of 3.45 V and 33 W h L^{-1}, respectively. Under flow conditions, the battery exhibited 81% capacity retention over 100 cycles with minimal active-material crossover, highlighting the robustness and scalability of the design (Fig. 6E).

These advancements underscore the potential of nonaqueous membrane-free RFBs to achieve higher energy densities and voltages, rendering them promising candidates for future large-scale energy-storage solutions. However, these systems have inherent drawbacks. The construction of such systems is challenging owing to the introduction of alkali metals, which require solvents with a high tolerance to low voltages, thus limiting the use of common solvents such as acetonitrile. Additionally, nonaqueous solvents generally have a lower ionic conductivity than water, thereby restricting most nonaqueous/nonaqueous membrane-free flow batteries from operating at low current densities.

3.2. Co-laminar flow batteries

The application of a single-phase co-laminar flow design in membrane-free electrochemical cells, such as fuel cells and flow batteries, represents an innovative approach.[18,43] Unlike the previously mentioned membrane-free batteries, the membrane-free mechanism in these cells is based on the characteristics of laminar flow (Fig. 7A). The formation of laminar flow is due to the dominance of viscous forces over inertial forces at low Reynolds numbers. This phenomenon causes fluid molecules to move along parallel streamlines and prevents significant mixing between fluids. The mathematical definition of the Reynolds number is

$$\mathrm{Re} = \rho U L / \mu$$

where ρ represents the density, μ is the dynamic viscosity, U is the average velocity of the fluid, and L is the characteristic length of the channel. When the Reynolds number is less than approximately 2000, the fluid tends to form laminar flow.[44]
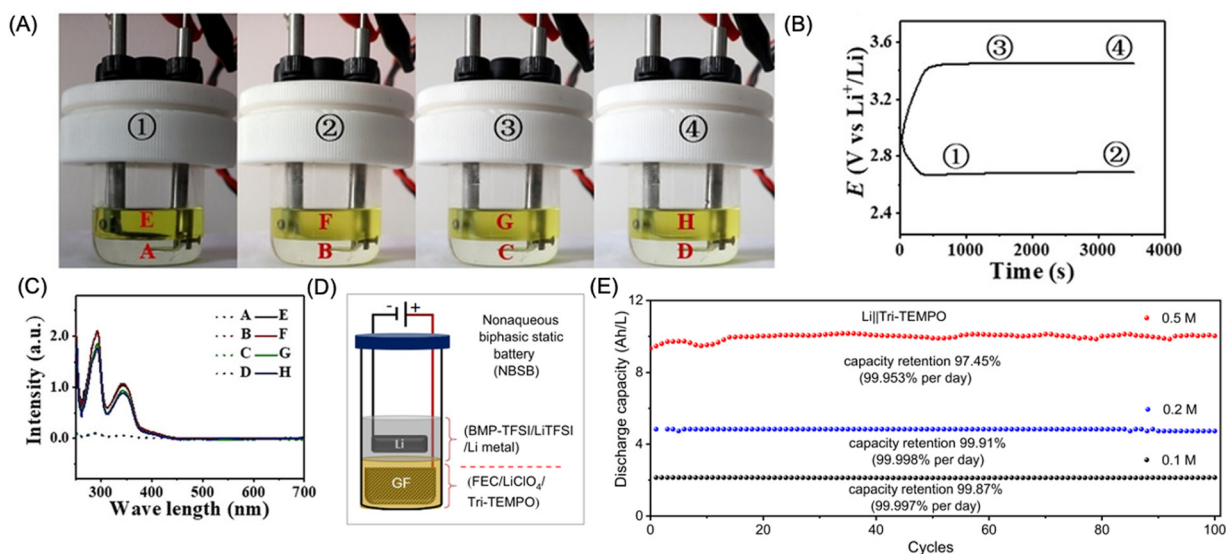

Fig. 6 *In situ* battery experiments using TEGDME and NFTOS as immiscible electrolytes. (A) Optical images at different charge–discharge stages, (B) corresponding charge–discharge curves, and (C) UV–visible spectra of TEGDME and NFTOS before and after cycling. Performance of Li‖Tri-TEMPO-based nonaqueous biphasic static batteries (NBSBs). (D) Schematic of NBSB[42] with a Li–metal anode in an anolyte solvent (BMP-TFSI/LiTFSI) and redox-active materials dissolved in the catholyte solvent (FEC). (E) Discharge capacities of the 0.1, 0.2, and 0.5 M Li‖Tri-TEMPO NBSBs. Reproduced with permission from ref. 41. Copyright 2024, John Wiley and Sons. Reproduced with permission from ref. 42. Copyright 2023, Springer Nature.
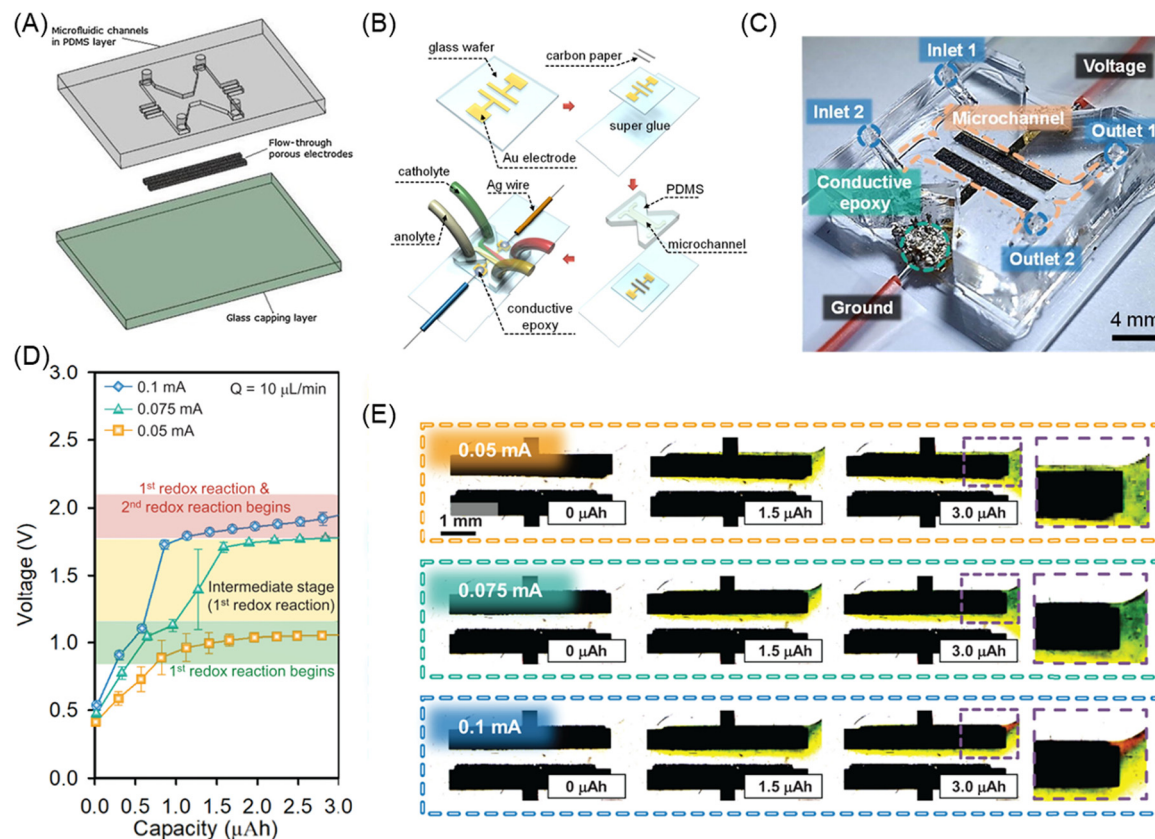
5902 | *Chem. Soc. Rev.*, 2025, **54**, 5895–5911

This journal is © The Royal Society of Chemistry 2025

Fig. 7 (A) Typical single-phase co-laminar flow battery. (B) Microscale fabrication process and (C) digital photograph of the microfluidic membrane-free RFB. (D) Voltage and capacity profiles of the membrane-free RFB using the redox couple in terms of charge transfer and (E) in *operando* visualization of the electrochemical reaction. Reproduced from ref. 43 with permission from the National Academy of Sciences, copyright 2022.

Therefore, the fluid channel geometry, flow velocity, fluid viscosity, and fluid density are the primary factors influencing laminar flow. The regulation of laminar flow is a critical aspect of maintaining efficient operation in membrane-free redox flow batteries (RFBs). Laminar flow ensures the stable separation of reactants, preventing mixing between the anolyte and catholyte and minimizing self-discharge. To achieve and sustain laminar flow, careful consideration of fluid dynamics principles is essential. The geometry of the flow channels, including their width, depth, and aspect ratio, significantly impacts the Reynolds number, which determines whether the flow remains laminar or transitions to turbulence.[45,46] Optimizing these dimensions is crucial for maintaining a laminar regime, particularly under varying flow rates and operational conditions. In addition, the viscosity and density of the electrolytes play vital roles in regulating flow behavior. By selecting electrolyte compositions with appropriate physical properties, the stability of the flow interface can be enhanced, ensuring effective reactant separation. Flow rate modulation is another key strategy, where precise control of the flow velocity helps maintain laminar conditions or selectively induces mixing at controlled interfaces to enhance reaction kinetics. Advanced techniques, such as computational fluid dynamics (CFD) simulations and experimental visualization, provide valuable tools for analyzing and optimizing flow patterns within membrane-free RFBs. These

methods enable the prediction and fine-tuning of flow behaviors, ensuring the system operates efficiently across a range of load conditions. Incorporating these insights into system design ensures the robust performance of membrane-free RFBs while leveraging their unique advantages.

In most studies, researchers have attempted to optimize these parameters to achieve a stable, low-crossover, and high ion-conductivity battery. However, due to the requirements for laminar flow within the cell channels, most co-laminar flow batteries are microfluidic flow batteries; thus, the overall cell volume is extremely small. This characteristic also changes the application scope and evaluation criteria. For example, microfluidic flow batteries are more suitable for specialized portable applications, such as lab-on-chip devices, rather than large-scale energy-storage systems.[47,48] Unlike conventional flow batteries, which are often assessed based on cycle life, microfluidic flow batteries place a greater emphasis on enhancing power density in terms of evaluation criteria.[19,49,50]

Single-phase co-laminar flow batteries employ laminar flow within the microchannels to maintain the separation of the anolyte and catholyte streams, which improves both the CE and energy density. An example of this design is the membrane-free H_2–Br_2 flow battery introduced by Braff *et al.*[51] The battery employs a membrane-free design that enables a power density of 0.795 W cm^{-2} at room temperature and atmospheric

This journal is © The Royal Society of Chemistry 2025

Chem. Soc. Rev., 2025, **54**, 5895–5911 | **5903**

pressure, with a round-trip voltage efficiency of 92% at a peak power of 25%. The cell uses a graphite cathode and commercial carbon cloth gas diffusion anode with a Pt catalyst, achieving high concentrations of both reactants at their respective electrodes and greatly expanding the mass-transfer capacity of the system. The use of gaseous H_2 fuel and aqueous Br_2 oxidant enables high-power-density storage and high-efficiency energy discharge while avoiding the cost and reliability issues associated with membrane-based systems. Their study marked a significant advancement in nonmembrane-based energy storage systems by demonstrating how laminar flow can effectively prevent reactant crossover without a physical barrier.

Further advancements in this area include a study published in 2022,[43] in which the researchers employed a membrane-free microfluidic platform for the *operando* visualization and analysis of RFBs. This innovative platform enabled the real-time observation of electrokinetic phenomena, which is crucial for understanding the intricate interactions between electrochemistry and hydrodynamics in RFBs. The platform utilized transparent materials, which enabled the direct visualization of the laminar flow interface and charge-transfer processes without the need for a membrane (Fig. 7B and C). By investigating the redox-active molecule 5,10-bis(2-methoxyethyl)-5,10-dihydrophenazine, which exhibits distinct color changes during redox reactions, the study provided valuable insights into the charge- and mass-transfer kinetics within the battery (Fig. 7C). These observations revealed the presence of rate-limiting regions and highlighted the importance of balancing charge- and mass-transfer rates to enhance battery performance. Numerical simulations were also conducted to further understand the physicochemical hydrodynamics behind battery operation. The simulations identified two critical regions affecting the performance: the diffusion region, where reactants diffused between phases; and the depletion region, in which the reactants were deficient (Fig. 7D and E). These findings suggest that optimizing the electrode geometry can mitigate the effects of these regions. By comparing a tapered electrode design with a traditional straight design, researchers demonstrated that the tapered electrode significantly reduced the overpotential and enhanced the efficiency of the redox reactions, resulting in improved battery performance. Their study underscored the potential of *operando* visualization techniques and numerical modeling to optimize the design and operation of membrane-free RFBs, rendering them promising for future research and applications in energy-storage systems. This visualization approach allows researchers to observe how charge transfer and flow rates interact dynamically, revealing the formation of depletion zones near the electrode that impact overall performance. The study uses both experimental data and numerical simulations to propose optimized electrode geometries that can reduce depletion effects and improve charge transfer efficiency, directly correlating geometric parameters with enhanced battery performance. Such real-time analysis tools, as demonstrated by Park *et al.*, are indispensable for characterizing complex interactions in membrane-free redox flow systems, where fluid dynamics and electrochemistry are tightly coupled.[43]

Current research on membrane-free microfluidic flow batteries primarily focuses on the structural design of the cells.

Based on the Reynolds number, certain approaches have potential feasibility. For example, the geometry of the fluid channel significantly influences the formation of laminar flow, with narrow channels promoting laminar flow by restricting the lateral movement of the fluid. Lower flow velocities help to sustain the laminar conditions and prevent turbulence. Fluids with higher viscosity are more likely to form laminar flows because viscous forces dominate, resulting in smoother patterns. Additionally, smooth and uniform fluid entry conditions help to establish and maintain laminar flow, while smoother channel walls reduce disturbances and enhance stability. In terms of active materials, there has been a shift from materials typically used in fuel cells, such as H_2 and Br, to inorganic metal materials such as vanadium acetylacetonate, and recently toward low-cost organic redox materials such as anthraquinone. In solvent systems, organic solvents have also been explored, resulting in the development of microscale redox batteries with high voltages and power densities of up to 2.6 V and 120 W cm^{-2}, respectively.

3.3. Other membrane-free flow battery systems

3.3.1. Liquid/solid membrane-free flow batteries. Liquid/solid membrane-free RFBs represent a novel class of energy-storage system (Fig. 8). The battery structure comprises a single-phase liquid electrolyte that flows over a solid-state electrode. (In this review, we exclude systems in which both electrodes are solid-state, as these configurations are more akin to fuel cells.)[52] This simple design eliminates the need for a membrane, resulting in a system with only one solid–liquid interface, and reduces both the complexity and cost of the battery, while potentially increasing its efficiency and longevity. One significant challenge of this system is that the reaction products, which are in a high-energy state, are in direct contact with each other. This results in simultaneous forward and reverse reactions, thereby affecting the CE of the battery.

Utilizing a co-laminar flow system, Suss and coworkers[53] introduced a membrane-free design that employed a multiphase flow system. Briefly, Zn metal was used as the anode and the electrolytes were prepared from a solution of $ZnBr_2$, Br_2, and *N*-ethyl-*N*-methylpyrrolidinium bromide, which equilibrated to form
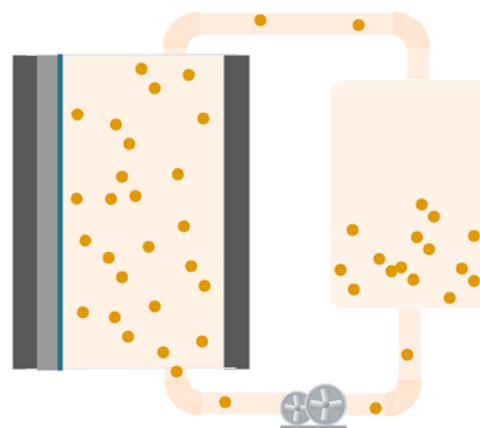

Fig. 8 Schematic illustration of liquid/solid membrane-free RFB.

5904 | *Chem. Soc. Rev.*, 2025, **54**, 5895–5911

This journal is © The Royal Society of Chemistry 2025

distinct aqueous and polybromide phases. The prototype cell demonstrated stable cycling performance with no significant capacity fade over ten cycles, and the voltaic efficiency and CE were 67% and 73%, respectively. This single- and multiphase-flow Zn–Br$_2$ RFB demonstrated significant potential for reducing the cost and complexity of energy storage systems. Their study introduced a clear path for future optimization, including improving the plating efficiency, enhancing the Br$_2$ storage capacity, and optimizing the flow dynamics to maximize performance.

Liao and colleagues[54] further explored this configuration with different forms of Zn anodes. They employed a homogeneous mixture of 1 M ZnCl$_2$ and 0.05 M hydroquinone in 2.5 M NaCl and 0.1 M HCl as the catholyte, in direct contact with the Zn anode. They found that varying the morphology of the Zn anode (plate, mesh, foam, and fiber) could improve the battery performance. In all tests, the CEs of the batteries were > 80%. Notably, the Zn fiber anode-equipped battery exhibited a superior energy efficiency of approximately 75% and retained 87% of its capacity after 100 cycles.

3.3.2. Triphasic membrane-free flow batteries. Triphasic membrane-free flow batteries are an emerging energy-storage technology. They employ three distinct phases to achieve efficient energy conversion and storage. In addition to the two phases functioning as solvents for the anode and cathode, a third phase is typically employed as a "membrane" phase. This is achieved through battery structure design and manipulation of the phase density (Fig. 9A, Design-I).[55] Triphasic membrane-free flow batteries have two primary designs. One approach leverages density differences to form upper, middle, and lower layers, with the middle layer functioning solely as an ion-conducting medium. For example, Kunitake and colleagues[56] utilized bi-continuous

microemulsions, aqueous NaCl, and CH$_2$Cl$_2$ as the middle, top, and bottom phases, respectively (Fig. 9B). They successfully constructed a liquid-membrane flow battery system by controlling the amount of surfactant. When anthraquinone and ferrocene were employed as the cathode and anode, respectively, the battery exhibited good stability in short-cycle tests. The second design involves placing a third phase at the top or bottom of two horizontally separated phases. Chakraborty et al.[57] adopted this design, using an aqueous phase as the top layer for ion transport and CH$_2$Cl$_2$ as the solvent for both the cathode and anode electrolytes, separated by glass (Fig. 9A, Design-II).

Compared to biphasic systems, the addition of a third phase in triphasic systems significantly inhibits crossover, resulting in a CE of > 99%, which surpasses that of most membrane-free battery systems. Despite these advantages, the system does not fully exploit the potential of the triphasic design. For example, the voltage of a $[Fc^+][PF_6^-]$||C7-PTZ system was only 0.81 V, which did not leverage the increased voltage range offered by the organic solvent (Fig. 9C).[56] In addition, impedance studies were conducted using an H-cell setup, which did not fully demonstrate the low-impedance advantage of the triphasic system. However, the CE of > 99% highlights the advantage of triphasic membrane-free flow batteries in addressing the rapid self-discharge and crossover issues of membrane-free batteries. These studies illustrate the potential of triphasic membrane-free flow batteries to enhance the energy storage efficiency and stability, offering significant improvements over biphasic systems. Liu et al. introduced a triphasic membrane-free RFB in an all-aqueous system, utilizing a salting-out approach with tetrabutylammonium chloride (TBACl) and Na$_2$SO$_4$ to form three immiscible aqueous phases.[58] Their
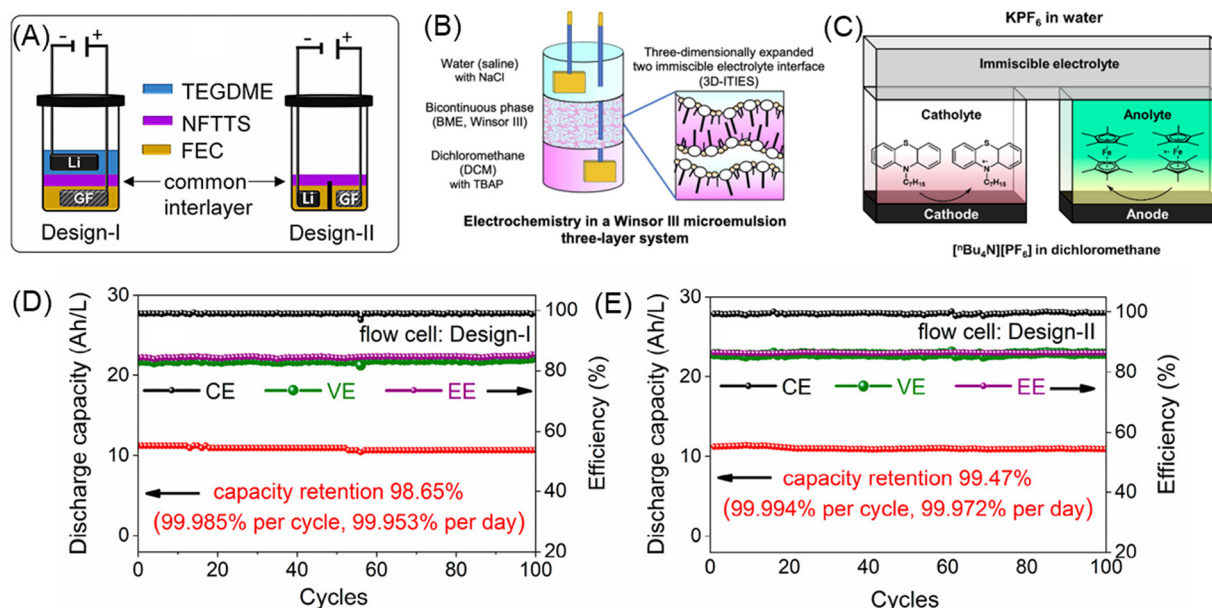

Fig. 9 (A) Schematic of triphasic systems (Design-I: top, middle, and bottom; and Design-II: top, left, and right). (B) Schematic of the triphasic bicontinuous microemulsion system. (C) Schematic of split triphasic system and redoxmer used. (D) and (E) Charge−discharge performance of Li||C18-PTZ (0.5 M) triphasic battery cells with (D) Design-I and (E) Design-II under flow conditions, including capacity retention, CE, voltage efficiency (VE), and energy efficiency (EE). Reproduced with permission from ref. 55. Copyright 2024, American Chemical Society. Reproduced with permission from ref. 56. Copyright 2023, Elsevier. Reproduced with permission from ref. 57. Copyright 2023, American Chemical Society.

This journal is © The Royal Society of Chemistry 2025

Chem. Soc. Rev., 2025, **54**, 5895–5911 | **5905**

design achieved stable operation over 360 cycles with an average Coulombic efficiency of 98.7% and minimal capacity decay (0.035% per cycle), demonstrating the potential of triphasic aqueous systems for high-performance membrane-free RFBs. In addition, Shao *et al.* present a pioneering triphasic membrane-free battery based on a salting-out effect, which utilizes metal-free redox materials.[59] This triphasic system separates the catholyte and anolyte with an immiscible electrolyte that serves as a stable interface, reducing crossover while achieving high Coulombic efficiency (above 99.5%) and negligible capacity decay over 660 cycles. By employing hydrogel as a support structure for the immiscible electrolyte, Liu *et al.* enhance the mechanical stability of the triphasic configuration and demonstrate compatibility with conventional RFB stacks. This approach addresses mechanical and chemical stability challenges in membrane-free battery designs and highlights the potential for high-capacity retention and extended cycling without the need for molecular modifications of redox-active materials. Their findings reinforce the viability of triphasic systems as sustainable, low-cost solutions in membrane-free flow battery technology.

Further advancements in the development of triphasic membrane-free nonaqueous RFBs have been achieved. Jiang's group[55] successfully assembled triphasic systems using two designs. In vertical Design-I, TEGDME, nonafluoro-1,1,2,2-tetrahydrohexyl-trimethoxysilane (NFTTS), and FEC were used as the anolyte, ionic conductive layer, and catholyte, respectively. In Design-II, NFTTS was placed on top as the conductive layer, with FEC serving as the solvent for both the anolyte and catholyte. Both designs, particularly Design-II, demonstrated success. Design-II was assembled with metallic Li as the anode and a phenothiazine derivative (C18-PTZ) as the cathode. The system exhibited high capacity retention ($\sim$98% over 31 days and 100 cycles under static conditions and $\sim$99% over 39 days and 100 cycles under flow conditions) and demonstrated an average CE of nearly 100% in both static and flow conditions (Fig. 9D). The cell leveraged the advantages of nonaqueous systems, achieving a cell voltage and solubility of 3.3 V and 0.5 M, respectively, which resulted in an energy density of above 40 W h L^{-1} under flow conditions. Thus, triphasic membrane-free systems represent a significant advancement in the field of redox flow and offer high efficiency, stability, and capacity retention. By addressing the limitations of biphasic systems, this approach holds great promise for the development of high-performance and cost-effective energy-storage solutions.

4. Parameters in membrane-free flow batteries

Compared with traditional flow batteries, membrane-free flow batteries have attracted attention owing to their unique cell architecture. The absence of a membrane enables direct contact between the reaction products of the anode and cathode, rendering self-discharge and CE critical parameters. Furthermore, the lack of a membrane introduces interface disturbances caused by

the flow of electrolytes, necessitating studies on interface resistance. These aspects are discussed in the following sections.

4.1. Coulombic efficiency and self-discharge

There are various strategies aimed at improving the efficiency and overall performance of membrane-free RFBs. Enhancing the CE of membrane-free RFBs is vital for practical applications. In microfluidic RFBs and metal-free aqueous-containing membrane-free flow battery systems, unavoidable self-discharge often results in CE values typically ranging from 70–90%, which are suboptimal.[18,24–26,50] This self-discharge arises from the direct contact between the reaction products of the anode and cathode. Approaches such as optimizing the flow rates and reactant concentrations can reduce the frequency of these contacts, thus improving the CE; however, these measures address only the symptoms rather than the underlying cause. In contrast, biphasic membrane-free flow batteries employing metal anodes generally exhibit higher CE values, with recent studies reporting CEs consistently above 96%.[30–32,42,60] Moreover, research on triphasic systems has demonstrated that innovative battery architectures can achieve CEs of >99%, significantly enhancing the performance of membrane-free batteries.[55,57]

4.2. Flow dynamics and management

As discussed in Section 3.2, the design of flow channels is crucial for the optimal performance of co-laminar flow RFBs. Continuous innovation in this area has resulted in the development of new models that enhance the control and stability of laminar flow within batteries.[50,61–63] In addition, they help to elucidate and predict the behavior of fluids within RFBs, enabling better design and operation strategies that minimize interface disturbances and maximize energy efficiency.

4.3. Flow rates

The optimization of flow rates is critical for improving the performance of membrane-free RFBs. Appropriate control of the flow rate can enhance the mixing of electrolytes, ensure a uniform distribution of reactants, and reduce the likelihood of self-discharge. Studies have demonstrated that varying the flow rate can significantly affect the overall efficiency and stability of battery systems. Higher flow rates may improve ion transport and reduce concentration polarization;[24] however, they also increase the risk of interfacial disturbances. This phenomenon occurs in both biphasic and triphasic systems, where the battery can operate stably but with compromised capacity utilization (Fig. 7).[31,55] Conversely, lower flow rates can maintain stable laminar flow but may not sufficiently support high current densities. Therefore, achieving an optimal flow rate balance is crucial for maximizing the performance of membrane-free RFBs. In co-laminar flow batteries, the impact of the flow rate on battery performance is more complex owing to its dependence on the Reynolds number.

4.4. Redoxmer

Designing redox-active materials with higher solubility and stability is particularly crucial, as these factors directly influence the energy density and Coulombic efficiency (CE) of the

5906 | *Chem. Soc. Rev.*, 2025, **54**, 5895–5911

This journal is © The Royal Society of Chemistry 2025

system. Redoxmers with enhanced solubility can store more energy per unit volume. High solubility can be achieved through several approaches, including molecular engineering of the redoxmer itself, the introduction of side-chain functional groups, and ionic effects. In membrane-free battery designs, these strategies remain applicable; however, the reliance on the physical immiscibility between the positive and negative electrolytes to prevent electrolyte mixing and crossover shifts the focus toward mutual solubility. For instance, in aqueous-nonaqueous systems, the active materials dissolved in the aqueous phase should exhibit high solubility in the aqueous medium but minimal solubility in the nonaqueous medium, and *vice versa*. This process can be described using the partition coefficient, $K = [\text{molecule}]_{\text{top phase}}/[\text{molecule}]_{\text{bottom phase}}$. Values of K greater than 1 indicate that the target molecule is preferentially dissolved in the top phase, whereas values less than 1 suggest that the target molecule predominantly partitions to the bottom phase. This provides theoretical guidance for the solubility distribution of redoxmers between the two phases. As for solubility itself, while the entire field of membrane-free batteries remains in an exploratory stage, and systematic efforts to enhance solubility in the context of membrane-free systems have not yet been established, the concentration of redoxmers in membrane-free batteries is gradually increasing with the discovery of new solvent/redoxmer systems.[29] Improving the stability of redoxmers can reduce degradation and support long-term cycling performance. As one of the most critical factors for battery performance, the stability considerations for membrane-free batteries are not vastly different from those of traditional flow batteries. However, the interaction between the two phases (despite phase separation, complete immiscibility is rarely achievable) significantly affects the redoxmer's stability, including both electrochemical and chemical stability. Wang *et al.*, using *operando* FT-IR spectroscopy, investigated the concentration changes of water in the organic phase of a biphasic system.[31] They observed that the water concentration in the organic phase peaked after approximately 13.8 hours and then levelized, providing evidence of mutual solubility in phase-separated systems. Based on this observation, they conducted electrochemical stability tests on two active materials in the presence of water. While TEMPO demonstrated insensitivity to water, another active material, PTZ, showed reduced stability due to the presence of water. Thus, when considering the stability of membrane-free batteries, the interactions between solvents across the phases should be factored into the design and optimization process.

4.5. Impedance studies

Interfacial resistance represents a crucial parameter influencing the performance of membrane-free RFBs. The absence of a membrane fundamentally alters the interfacial kinetics, thereby making impedance studies indispensable for a comprehensive understanding of resistance-related losses and for developing effective mitigation strategies. In traditional RFBs, the overall impedance is predominantly governed by the resistance of the membrane. However, in membrane-free systems, this paradigm shifts, and the impedance is instead dominated by the transport resistance within the electrolyte solutions. This transition is clearly reflected in the area-specific resistance (ASR) contributions (less than 50% in membrane-free system and over 70% in other aqueous redox flow batteries) observed in membrane-free battery systems.[24]

Previous investigations into the impedance behavior at liquid–liquid interfaces have demonstrated that interfacial resistance does not constitute the rate-limiting step in the overall impedance system.[64] A similar conclusion has been reached in recent studies focusing on membrane-free batteries, further supporting this observation.[42] To gain deeper insights into the impedance behavior at the liquid–liquid interface, the authors conducted a series of targeted experiments. They individually measured the impedance responses of FEC and BMP-TFSI electrolytes while maintaining fixed parameters for these electrolyte systems during the fitting process to ensure consistency and accuracy. This meticulous approach enabled them to accurately quantify the impedance at the liquid–liquid interface. The results revealed that the charge transfer resistance in the bulk organic phase exceeds 100 Ω, whereas the impedance at the liquid–liquid interface is approximately 10 Ω. These findings indicate that, despite the absence of a membrane, the liquid–liquid interface does not serve as a primary bottleneck for the overall performance of the system, highlighting the robustness of this interface in supporting efficient battery operation.''

4.6. Electrolyte system selection

An ideal electrolyte system for membrane-free batteries must satisfy the following conditions: (1). Stable biphasic system: the system should form a stable biphasic configuration to ensure both electrochemical and chemical stability at the liquid–liquid interface where ion transport occurs. (2). Density difference: the two liquid phases should have different densities, allowing the electrolyte to spontaneously separate into distinct phases under gravitational forces. (3). Shared ions: the two phases must share common ions to facilitate ion transport during battery operation. (4). High ionic conductivity: the electrolyte system should exhibit high ionic conductivity to ensure optimal battery performance. In early-stage membrane-free battery development, electrolyte systems were often designed based on empirical rules. For example, a greater difference in dielectric constants between two liquids generally indicates lower mutual solubility. Alternatively, researchers relied on trial-and-error methods or borrowed concepts from existing aqueous two-phase systems.[65] However, to date, no unified parameter exists to precisely describe the mutual solubility of two liquids, especially in the context of electrolytes, where the addition of salts further complicates the system and makes analysis more challenging. The Hansen solubility parameters (HSP) offer a more comprehensive framework for predicting the miscibility and stability of different solvent combinations. By mapping solvents in a three-dimensional space defined by dispersion, polarity, and hydrogen-bonding interactions, the HSP model allows predictions of which solvents might form stable biphasic systems. Solvents that are close in this parameter space are likely to be

This journal is © The Royal Society of Chemistry 2025

Chem. Soc. Rev., 2025, **54**, 5895–5911 | **5907**

miscible, while those far apart can form distinct, immiscible layers suitable for constructing biphasic systems. However, as Hansen himself notes on his website,[66,67] the HSP model is more suited for describing large molecular compounds and may lack accuracy when applied to small-molecule solvents. Consequently, further research is needed to develop a clear and concise parameter for describing mutual solubility in electrolyte systems. Such a parameter would provide invaluable guidance for designing and optimizing membrane-free battery systems.

In addition to phase separation caused by the intrinsic properties of solvents, another common mechanism for phase separation is the salting-out effect. The salting-out effect refers to the phenomenon where the addition of salts to a solution induces phase separation between two liquid solvents. Fundamentally, the salting-out effect arises from the salt altering the properties of the solvent, weakening the interactions between the solute and the solvent, thereby promoting the formation of a biphasic system. The salting-out effect is often described by the Setschenow equation: $\text{Log}(S/S_0) = k_s \times [\text{salt}]$. Here, in biphasic systems, [salt] represents the solubility of the second solvent in the first solvent. However, while the Setschenow equation provides a parameter to describe the extent of the salting-out effect, it has limited practical value in guiding the formation of biphasic systems. The strength of the salting-out effect can be qualitatively assessed using the Hofmeister series, which offers more practical reference for real-world applications. For example: strong salting-out ions: SO_4^{2-} and Na^+; weak salting-out ions (anti-salting-out): I^-, SCN^-, and NH_4^+. A representative example is the work by Meng et al.,[29] where 1.8 M $MgSO_4$ was used to induce phase separation between TEGDME and water.

4.7. Cost

While numerous RFB systems have been analyzed on cost, most of these analyses are limited to the laboratory scale, focusing primarily on key components such as active materials, electrolytes, and membranes. This approach offers a limited perspective, emphasizing the necessity of detailed and realistic cost estimations that better reflect industrial-scale applications.

To address this gap, Sprenkle et al. developed a cost estimation model for redox flow batteries that incorporates more practical factors, such as pump losses and shunt currents. Building on this foundation, L. Tang et al. proposed a more comprehensive cost model that considers raw active materials, solvents, battery components, and the performance of various well-known chemistries based on different architectures.[68] We adopt the latter model and conduct a detailed cost analysis of membrane-free battery designs, using the system described in Jiang's work as a representative case.[17]

Given the lack of commercially successful membrane-free RFB systems, we will adapt the cost model used for Regenesys® modules for a 2 MW × 6 h all-vanadium batteries,[69,70] as a baseline, with adjustments to account for the unique characteristics of membrane-free systems. In this model, the total cost of a RFB is simplified into three major components: the cell stack (including electrodes, membranes, gaskets, and bolts), the electrolyte (comprising active materials, salts, and solvents),

and balance of plant equipment (such as tanks, pumps, heat exchangers, condensers, and rebalance cells), along with the power conversion system (PCS).

For membrane-free designs, the elimination of the membrane reduces the cost. In addition, due to the immiscibility of the positive and negative electrolytes, the need for rebalance operation for common Vanadium RFB is also negated.[71] However, due to the absence of large-scale industrial applications, we will not account for potential reductions in the use of traditional gaskets (typically PTFE or PVC frames) or any increase in the use of transparent gaskets (usually glass). We used this approach to calculate the cost of the batteries described in previous membrane-free study (Table 2).

A comparative analysis of the cost components between traditional systems and the membrane-free design, based on example 1 and example 2 from the Tables 2 and 3, underscores this advantage. The total cost for example 1 is USD$ 135.57 per kW h, while for example 2 (both examples being membrane-free RFBs), it is USD$ 116.58 per kW h. In comparison, the all-V system has a total cost of USD$ 251.88 per kW h, indicating that the membrane-free design achieves a cost reduction of approximately 45–50%. This reduction is primarily attributed to the elimination of membrane costs and the simplification of system components, such as the

Table 2 Summaries of cost for some typical RFBs systems in application 1 of 2 MW × 6 h^{a}.[68–70]

RFB	All-V	Zn–Br	Zn–Fe(CN)$_6$	AQ–Br	Vi-TEMPO
Cost ($ per kW h)	251.88	435.73	413.55	308.34	517.84

RFB	Ph–Fe(CN)$_6$	FL-DBMMB	All-metallocene	Li-TEMPO	Zn-TEMPO
Cost ($ per kW h)	168.40	1549.11	6751.11	1236.60	116.58

^{a} Due to the absence of commercially successful membrane-free RFB systems, we will use the cost model developed for Regenesys® modules as a baseline for a 2 MW × 6 h all-vanadium battery,[69,70] incorporating modifications to reflect the distinct features of membrane-free designs.

Table 3 Summaries of cost for some membrane-free RFBs systems in 2 MW × 6 h storage applications

Cost (USD per kW h)

Component	Example 1[72]	Example 2[31]	Example 3[42]
Bipolar plate	23.76	11.03	11.03
Graphite felt	32.93	30.58	30.58
PVC frame	7.15	3.32	3.32
Membrane	0	0	0
Gaskets, bolts, end-plate	11.98	5.56	5.56
Pump	1.05	0.98	0.98
Battery management system	3.25	1.51	1.51
Heat exchanger	14	14	14
Electrolyte tank	26.29	2.64	2.64
Rebalance cell	1.38	2.07	2.07
Solvent	0.86	26.05	94.33
Condensor	0	0	0
Active materials	12.38	10.01	44.15
Salt	0.54	10.81	257.14
Total	135.5726	116.58	467.31

5908 | Chem. Soc. Rev., 2025, **54**, 5895–5911

This journal is © The Royal Society of Chemistry 2025

rebalance cell. The cost of critical components such as the bipolar plate and graphite felt remains comparable in both designs, indicating that the cost advantage of the membrane-free system is not at the expense of other essential materials. However, it is essential to note that the absence of large-scale industrial applications for membrane-free systems introduces certain limitations to this analysis. Potential cost reductions from reduced usage of traditional gaskets (*e.g.*, PTFE or PVC frames) or increased use of alternative materials such as glass-based gaskets were not accounted for. This conservative approach ensures the reported cost advantages are realistic and not overly optimistic. In example 3, although it operates at a higher voltage and supports multi-electron transfer, which reduces the cost of redoxmers, the use of organic solvents and the application of high-cost salts compatible with these solvents diminish its overall cost-effectiveness.

In conclusion, membrane-free RFB designs demonstrate clear cost benefits over traditional membrane-based systems. These cost advantages, coupled with the potential for further optimization through material innovation and scalability, position membrane-free designs as a promising solution for cost-effective energy storage. For instance, scaling the modeled application from 2 MW × 6 h to a larger system, such as 10 MW × 11 h, could further reduce the overall cost of the battery stack due to economies of scale. Identifying such practical improvements through comprehensive cost assessments not only facilitates the development of more efficient systems but also contributes to reducing costs. This progress aligns with the U.S. Department of Energy's (DoE) long-term goal of achieving battery market costs below 100 USD $(kW\ h)^{-1}$.

4.8. Other parameters

Beyond CE and flow dynamics, other important parameters include energy and power density, cycle life and stability, self-discharge rate, interface resistance, and cost. Each factor plays a critical role in the performance and economic feasibility of membrane-free RFBs. Enhancing these parameters can significantly improve the competitiveness of these batteries in the energy-storage market. By focusing on comprehensive optimization strategies, membrane-free RFBs can be developed into highly efficient and cost-effective energy-storage solutions suitable for a wide range of applications.

5. Overall conclusions and perspectives

The review provides a comprehensive overview of the fundamental design principles, existing categories, and architectures of membrane-free RFB systems, offering a critical and timely summary of their development, while highlighting the unique design aesthetics behind this technology. Membrane-free RFBs have represented a groundbreaking innovation in the field of chemical energy storage over the past decade. They hold promise for next-generation large-scale green-energy storage systems owing to their simple structure, flexible design, and high compatibility with intermittent renewable energy sources.

Over the past five years, the proof-of-concept for membrane-free RFB began with aqueous biphasic electrolyte systems and rapidly expanded to aqueous/nonaqueous hybrid and nonaqueous biphasic systems. Despite these advancements, several critical challenges remain for their commercial adoption. Scalability involves modular cell configurations that can enhance flexibility for large-scale applications by allowing adjustments in cell numbers and flow rates to meet diverse energy demands, particularly in grid-scale energy storage. Challenges remain in manufacturing precision reactor cells to manage fluid control effectively without a membrane. Material cost and availability pose obstacles for scaling up, necessitating sustainable and recyclable electrode and electrolyte materials. Adaptive power electronics and control systems are also essential to integrate these batteries with fluctuating renewable energy inputs. Long-term stability is a pressing issue, with factors such as electrolyte decomposition, contamination, and material durability playing critical roles. Strategies such as periodic electrolyte refreshing, stabilizing additives, and corrosion-resistant materials (*e.g.*, carbon-based electrodes, protective surface coatings) can mitigate degradation. Maintaining stable laminar flow under real-world temperature and pressure fluctuations requires optimized flow rates, channel design, and viscosity control. Environmental impact assessments reveal significant ecological considerations for large-scale deployment. The use of recyclable and environmentally friendly materials, such as water-based electrolytes and renewable electrode components, can reduce waste. Exploring biodegradable materials further minimizes environmental footprints. Membrane-free RFBs offer the potential to reduce carbon emissions when integrated with renewable energy sources due to their high energy efficiency and reduced reliance on fossil fuel-based power systems. By addressing these challenges and leveraging their inherent design advantages, membrane-free RFBs hold significant potential as cost-effective, scalable, and sustainable energy storage solutions for future applications. Continued research and development focusing on these aspects will be essential to bridge the gap from laboratory innovation to practical commercialization.

However, despite their numerous advantages, membrane-free RFBs face several unique challenges, such as reactant mixing and maintaining stable interfaces under high flow rates over extended periods. A primary challenge is in ensuring the long-term stability of the system without a physical membrane to prevent crossover. Innovative strategies, such as using immiscible electrolyte pairs and advanced fluid dynamics, are being explored to address these challenges. Additionally, the material selection for electrodes and electrolytes is crucial for enhancing the overall performance and durability of these batteries. Possible optimization directions require serious consideration in future research and development to bridge the gap from research to practical applications.

Although membrane-free RFBs avoid the need for expensive and fragile membranes, their cycle lives remain unsatisfactory, particularly the crucial parameter of calendar life, which is essential for large-scale energy storage. Certain systems undergo spontaneous reactions at the phase interface owing to dissolved and enriched cathode and anode materials, resulting in poor

This journal is © The Royal Society of Chemistry 2025

Chem. Soc. Rev., 2025, **54**, 5895–5911 | **5909**

charge retention. Systems using metal foils as electrode materials can avoid these reactions; however, they face structural collapse risks, particularly without external pressure, to prevent arbitrary dendrite growth. Additionally, the current concentrations of the active species in membrane-free RFBs are lower (generally <1 M) than those in conventional RFBs, resulting in relatively low output potentials. Achieving higher concentrations often require solvents with large dielectric constants, which are typically limited by their narrow electrochemical windows. The migration of charge carriers at the phase interface during charging or discharging requires the interface barriers to be overcome owing to differences in chemical potential, thereby reducing the overall energy density and efficiency of the system. Using heterogeneous electrolytes in these systems has also shown potential for enhancing conventional battery performance; however, it is typically validated in single-layer cells and is not yet compatible with practical multilayer batteries. Gelling the electrolyte phases to achieve location fixation in stacked batteries can ensure the full advantage of membrane-free flow battery systems. Unlike the current Li-ion batteries, membrane-free flow battery systems resemble unique large-scale chemical engineering reaction devices that are influenced by multiple parameters. Further development of their chemistry and engineering is ongoing and requires combined efforts in fundamental studies, materials development, and systems engineering.

Data availability

This is a review article summarizing the recent progress of the membrane-free redox flow batteries. This is not a research-based article; thus, research data is unavailable.

Conflicts of interest

There are no conflicts to declare.

Acknowledgements

References

1 G. Zichittella and J. Pérez-Ramírez, *Chem. Soc. Rev.*, 2021, **50**, 2984–3012.

2 H. Ji, J. Wang, J. Ma, H.-M. Cheng and G. Zhou, *Chem. Soc. Rev.*, 2023, **52**, 8194–8244.

3 G. Gowrisankaran, S. S. Reynolds and M. Samano, *J. Political Econ.*, 2016, **124**, 1187–1234.

4 Y. Zhou, S. Zhang, Y. Ding, L. Zhang, C. Zhang, X. Zhang, Y. Zhao and G. Yu, *Adv. Mater.*, 2018, **30**, e1802294.

5 H. Meng, S. Pang and G. Cui, *ChemSusChem*, 2019, **12**, 3431–3447.

6 K. Heussen, S. Koch, A. Ulbig and G. Andersson, *IEEE Sens. J.*, 2012, **6**, 140–151.

7 M. E. Baran, S. Teleke, L. Anderson, A. Huang, S. Bhattacharya and S. Atcitty, *STATCOM with energy storage for smoothing intermittent wind farm power*, Pittsburgh, PA, USA, 2008.

8 J. R. Gouveia, E. Silva, T. M. Mata, A. Mendes, N. S. Caetano and A. A. Martins, *Energy Rep.*, 2020, **6**, 87–94.

9 Y. Ding, C. Zhang, L. Zhang, Y. Zhou and G. Yu, *Chem. Soc. Rev.*, 2018, **47**, 69–103.

10 X. Wei, W. Pan, W. Duan, A. Hollas, Z. Yang, B. Li, Z. Nie, J. Liu, D. Reed, W. Wang and V. Sprenkle, *ACS Energy Lett.*, 2017, **2**, 2187–2204.

11 X. Fang, Z. Li, Y. Zhao, D. Yue, L. Zhang and X. Wei, *ACS Mater. Lett.*, 2022, 277–306.

12 F. R. Brushett, M. J. Aziz and K. E. Rodby, *ACS Energy Lett.*, 2020, **5**, 879–884.

13 P. Xiong, L. Zhang, Y. Chen, S. Peng and G. Yu, *Angew. Chem., Int. Ed.*, 2021, **60**, 24770–24798.

14 Z. Yuan, H. Zhang and X. Li, *Chem. Commun.*, 2018, **54**, 7570–7588.

15 P. Navalpotro, J. Palma, V. Muñoz-Perales, A. Martínez-Bejarano, M. V. Martín-Arroyo, D. P. Taylor, A. Platek-Mielczarek, P. G. Rivano, F. Paratore, E. D. Re and R. Marcilla, *APL Energy*, 2025, **3**, 1–6.

16 M. E. Suss, K. Conforti, L. Gilson, C. R. Buie and M. Z. Bazant, *RSC Adv.*, 2016, **6**, 100209.

17 P. Navalpotro, J. Palma, M. Anderson and R. Marcilla, *Angew. Chem., Int. Ed.*, 2017, **56**, 12460–12465.

18 M. O. Bamgbopa, S. Almheiri and H. Sun, *Renewable Sustainable Energy Rev.*, 2017, **70**, 506–518.

19 N. Chaabene, K. Ngo, M. Turmine and V. Vivier, *J. Energy Storage*, 2023, **57**, 106270.

20 Z. Wang, H. Ji, J. Zhou, Y. Zheng, J. Liu, T. Qian and C. Yan, *Nat. Commun.*, 2023, **14**, 2267.

21 J. Winsberg, T. Hagemann, T. Janoschka, M. D. Hager and U. S. Schubert, *Angew. Chem., Int. Ed.*, 2017, **56**, 686–711.

22 X. Z. Yuan, C. Song, A. Platt, N. Zhao, H. Wang, H. Li, K. Fatih and D. Jang, *Int. J. Energy Res.*, 2019, **43**, 6599–6638.

23 A. G. Olabi, M. A. Allam, M. A. Abdelkareem, T. Deepa, A. H. Alami, Q. Abbas, A. Alkhalidi and E. T. Sayed, *Batteries*, 2023, **9**, 409.

24 P. Navalpotro, C. Neves, J. Palma, M. G. Freire, J. A. P. Coutinho and R. Marcilla, *Adv. Sci.*, 2018, **5**, 1800576.

25 P. Navalpotro, C. Trujillo, I. Montes, C. M. S. S. Neves, J. Palma, M. G. Freire, J. A. P. Coutinho and R. Marcilla, *Energy Storage Mater.*, 2020, **26**, 400–407.

26 P. Navalpotro, S. E. Ibañez, E. Pedraza and R. Marcilla, *Energy Storage Mater.*, 2023, **56**, 403–411.

27 K. Gong, F. Xu, M. G. Lehrich, X. Ma, S. Gu and Y. Yan, *J. Electrochem. Soc.*, 2017, **164**, A2590–A2593.

28 M. O. Bamgbopa, Y. Shao-Horn, R. Hashaikeh and S. Almheiri, *Electrochim. Acta*, 2018, **267**, 41–50.

29 J. Meng, Q. Tang, L. Zhou, C. Zhao, M. Chen, Y. Shen, J. Zhou, G. Feng, Y. Shen and Y. Huang, *Joule*, 2020, **4**, 953–966.

30 J. Chai, A. Lashgari, A. E. Eisenhart, X. Wang, T. L. Beck and J. J. Jiang, *ACS Mater. Lett.*, 2021, **3**, 337–343.

31 X. Wang, A. Lashgari, J. Chai and J. J. Jiang, *Energy Storage Mater.*, 2021, **45**, 1100–1108.

5910 | *Chem. Soc. Rev.*, 2025, **54**, 5895–5911

This journal is © The Royal Society of Chemistry 2025

32 H. Yang, S. Lin, Y. Qu, G. Wang, S. Xiang, F. Liu, C. Wang, H. Tang, D. Wang, Z. Wang, X. Liu, Y. Zhang and Y. Wu, *Adv. Sci.*, 2024, **11**, 2307780.

33 S. T. Senthilkumar, S. E. Ibañez, P. Navalpotro, E. Pedraza, N. Patil, J. Palma and R. Marcilla, *J. Power Sources*, 2024, **608**, 234660.

34 G. Li, W. Chen, H. Zhang, Y. Gong, F. Shi, J. Wang, R. Zhang, G. Chen, Y. Jin, T. Wu, Z. Tang and Y. Cui, *Adv. Energy Mater.*, 2020, **10**, 1902085.

35 A. Ejigu, A. Elgendy, H. A. Al Nasser, K. Jupp and R. A. W. Dryfe, *Electrochim. Acta*, 2025, **512**, 145426.

36 A. Bayaguud, Y. Fu and C. Zhu, *J. Energy Chem.*, 2022, **64**, 246–262.

37 S. Hou, L. Chen, X. Fan, X. Fan, X. Ji, B. Wang, C. Cui, J. Chen, C. Yang and W. Wang, *Nat. Commun.*, 2022, **13**, 1281.

38 R. K. Gautam, J. J. McGrath, X. Wang and J. J. Jiang, *J. Am. Chem. Soc.*, 2024, **164**, 28414–28426.

39 H. Zhang, Y. Cheng, D. G. Lek, T. Liu, F. Lin, W. Luo, S. Huang, M. Gao, X. Wang and Y. Zhi, *J. Power Sources*, 2022, **548**, 232081.

40 Y. Ren and A. Manthiram, *Adv. Energy Mater.*, 2022, **12**, 2202566.

41 X. Liu, X. Song, Z. Guo, T. Bian, J. Zhang and Y. Zhao, *Angew. Chem., Int. Ed.*, 2021, **60**, 16360–16365.

42 R. K. Gautam, X. Wang, A. Lashgari, S. Sinha, J. McGrath, R. Siwakoti and J. J. Jiang, *Nat. Commun.*, 2023, **14**, 4753.

43 H. Park, G. Kwon, H. Lee, K. Lee, S. Y. Park, J. E. Kwon, K. Kang and S. J. Kim, *Proc. Natl. Acad. Sci. U. S. A.*, 2022, **119**, e2114947119.

44 A. Kumar and U. Panda, in *Biosensor Based Advanced Cancer Diagnostics*, ed. R. Khan, A. Parihar and S. K. Sanghi, Academic Press, 2022, pp. 197–224, DOI: 10.1016/B978-0-12-823424-2.00011-9.

45 T. Wei and W. Willmarth, *J. Fluid Mech.*, 1989, **204**, 57–95.

46 G. Sofiadis and I. Sarris, *Phys. Fluids*, 2022, **34**, 075126.

47 S. A. Mousavi Shaegh, N.-T. Nguyen and S. H. Chan, *Int. J. Hydrogen Energy*, 2011, **36**, 5675–5694.

48 J. W. Lee, M. A. Goulet and E. Kjeang, *Lab Chip*, 2013, **13**, 2504–2507.

49 B. Oraá-Poblete, D. Perez-Antolin, A. A. Maurice, J. Palma, E. Kjeang and A. E. Quintero, *Batter. Supercaps*, 2023, **7**, e202300367.

50 D. Alfisi, A. N. Shocron, R. Gloukhovski, D. A. Vermaas and M. E. Suss, *ACS Sustainable Chem. Eng.*, 2022, **10**, 12985–12992.

51 W. A. Braff, M. Z. Bazant and C. R. Buie, *Nat. Commun.*, 2013, **4**, 2346.

52 Y. Cheng, N. Zhang, Q. Wang, Y. Guo, S. Tao, Z. Liao, P. Jiang and Z. Xiang, *Nano Energy*, 2019, **63**, 103822.

53 L. Amit, D. Naar, R. Gloukhovski, J. la O' G and M. E. Suss, *ChemSusChem*, 2021, **14**, 1068–1073.

54 L. Tang, S. Dai, P. Leung, M. R. Mohamed, Y. Zeng, X. Zhu, C. Flox, A. A. Shah and Q. Liao, *Batteries*, 2023, **9**, 340.

55 R. K. Gautam, X. Wang, S. Sinha and J. J. Jiang, *ACS Energy Lett.*, 2023, **9**, 218–225.

56 K. Nakao, K. Noda, H. Hashimoto, M. Nakagawa, T. Nishimi, A. Ohira, Y. Sato, D. Kato, T. Kamata, O. Niwa and M. Kunitake, *J. Colloid Interface Sci.*, 2023, **641**, 348–358.

57 A. Chakraborty, R. Bock, R. Green, K. Luker, G. Ménard and L. Sepunaru, *ACS Appl. Energy Mater.*, 2022, **6**, 605–610.

58 J. Liu, J. Deng, Y. Hua, C. Liu, X. Zhang, M. Li and Y. Shao, *ACS Appl. Energy Mater.*, 2024, **7**, 12131–12140.

59 J. Liu, J. Wu, Z. Huang, M. Zhou, Y. Hu, X. Zhang, X. Shi, H. Zhou, M. Li and Y. Shao, *Energy Storage Mater.*, 2024, **70**, 103467.

60 W.-Y. Kim, H.-I. Kim, K. M. Lee, E. Shin, X. Liu, H. Moon, H. Adenusi, S. Passerini, S. K. Kwak and S.-Y. Lee, *Energy Environ. Sci.*, 2022, **15**, 5217–5228.

61 M.-A. Goulet and E. Kjeang, *Electrochim. Acta*, 2014, **140**, 217–224.

62 K. M. Lisboa and R. M. Cotta, *Appl. Math. Model.*, 2020, 77, 1512–1530.

63 A. B. D. Quirós, A. E. Quintero, A. Francés, A. A. Maurice and J. Uceda, *IEEE Access*, 2023, **11**, 46132–46143.

64 J. Akilavasan and F. Marlow, *J. Phys. Chem. C*, 2020, **124**, 4101–4108.

65 J. F. Pereira, M. G. Freire and J. A. Coutinho, *Fluid Phase Equilib.*, 2020, **505**, 112341.

66 https://www.hansen-solubility.com/HSP-science/small_solutes.php.

67 M. J. Louwerse, A. Maldonado, S. Rousseau, C. Moreau-Masselon, B. Roux and G. Rothenberg, *ChemPhysChem*, 2017, **18**, 2999–3006.

68 L. Tang, P. Leung, M. R. Mohamed, Q. Xu, S. Dai, X. Zhu, C. Flox, A. A. Shah and Q. Liao, *Electrochim. Acta*, 2023, **437**, 141460.

69 P. Leung, D. Aili, Q. Xu, A. Rodchanarowan and A. A. Shah, *Sustainable Energy Fuels*, 2018, **2**, 2252–2259.

70 R. M. Darling, K. G. Gallagher, J. A. Kowalski, S. Ha and F. R. Brushett, *Energy Environ. Sci.*, 2014, **7**, 3459–3477.

71 N. Poli, A. Trovò, P. Fischer, J. Noack and M. Guarnieri, *J. Energy Storage*, 2023, **58**, 106404.

72 P. Leung, T. Martin, A. A. Shah, M. R. Mohamed, M. A. Anderson and J. Palma, *J. Power Sources*, 2017, **341**, 36–45.

This journal is © The Royal Society of Chemistry 2025

Chem. Soc. Rev., 2025, **54**, 5895–5911 | 5911